Supplementary Materials

RNA Isolation and Size Fractionation

Endobronchial biopsies were immediately snap-frozen and stored at -80 °C. RNA was extracted from bronchial biopsies by using the miRNeasy mini kit (QIAGEN) according to manufacturer's protocol. The purity of RNA fractions was checked on NanoDrop 1000 UV-Vis spectrophotometer. The RNA integrity was verified using RNA 6000 Pico Assay RNA chips run in Agilent 2100 Bioanalyzer (Agilent Technologies, Palo Alto, CA).

RNA processing and microarray hybridization

All procedures were performed at Boston University Microarray Resource Facility as described in FlashTag™ Biotin HSR Labeling Kit (Affymetrix, Santa Clara, CA, current version available at www.affymetrix.com). The Qiagen miRNeasy Mini Kit and RNeasy MinElute Cleanup Kit were used to isolate small fractions of RNA.

Statistical model for the identification of miRNAs differentially expressed between ICS treatment and placebo over 6 and 30 months.

A linear mixed effects model was used with treatment defined as a categorical variable with two levels: treatment with ICS versus placebo (R_statistical_software_V3.0.2). Time was defined as a categorical variable with three levels: baseline, 6- and 30-month. The model was adjusted for the following confounding variables: RNA integrity number (RIN), smoking status, age and gender with patient ID as random effect variable. The model was structured as follows:

$$Me_{ij} = \beta_0 + \beta_1 X_{RIN-i} + \beta_2 X_{Smoking\_Status-i}$$

$$+ \beta_3 X_{Age-i} + \beta_4 X_{Gender-i} + \beta_5 X_{Treatment-i}$$

$$+ \beta_6 X_{Time-i} + \beta_7 X_{Treatment-i:Time-i} + \varepsilon_{ij} + \alpha_j$$

In this model, Me is the log2 microRNA expression for each miRNA for sample i from patient j, ε_{ij} represents error that is assumed to be normally distributed and α_j represents the patient random effect. The coefficients from the interaction term $\beta_7 X_{Treatment-i:Time-i}$ from the linear mixed effects model was used to select miRNAs which significantly changed in the same direction after 6 and 30 months of ICS treatment versus placebo. Using a linear mixed effects model, no miRNA passed the FDR<0.25 level. We therefore decreased our cut off level to nominal p<0.05.

To determine whether alterations of inflammatory cell populations were responsible for the miRNA expression changes during treatment, we adjusted for changes in numbers of neutrophils, eosinophils, macrophages, mast cells and epithelial cells in bronchial biopsies in a separate analysis.

Independent Cohort

To determine the relationship between microRNA expression associated with long-term fluticasone use and microRNA expression profiles associated with COPD-related decreases in lung function, we examined an independent dataset of microRNA profiling from airway brushing samples obtained from individuals with (n=32) and without (n=32) COPD at the British Columbia Cancer Agency. This cohort and sample processing methods have been been previously described (1).

Low-molecular weight RNA isolated from these bronchial brushings was profiled using the Illumina HiSeq 2000. Following library preparation with the TruSeq Small RNA Sample Prep Kit (Illumina), RNA adapters were ligated, the products reverse transcribed, and the resulting cDNA PCR-amplified using a six-base index tag to allow multiplexing of samples within a single flowcell lane. Six index-tagged PCR-enriched cDNA libraries were pooled, gel purified, and loaded into a single flowcell lane for cBot cluster generation using the TruSeq Single-Read Cluster Kit (Illumina). The flowcell was then sequenced using the Illumina HiSeq2000. Sequencing files were de-multiplexed and adapters trimmed using CASAVA and FastXClipper, respectively. We aligned sequences 15-100 base-pairs in length to hg19 using Bowtie, and annotated these reads using mirBase v18. A total of 4 samples were excluded based on quality metrics, leaving airway brushing microRNA-Seq data from 30 participants with COPD and 30 participants without COPD. After excluding microRNA with fewer than 20 counts per sample, we evaluated the association of microRNA expression with FEV1% using a linear model adjusting for age, sex, smoking status, and pack-years of smoking as previously described. The replication of the ICS effects focused on the subset of COPD patients with known ICS status comparing ICS usage (n=6) to no ICS (n=24). The analysis was conducted using a linear model correcting for pack years.

GSEA Analysis

GSEA analysis was then used to confirm that negatively correlated miRNA predicted targets were altered following ICS treatment. This analysis was conducted by comparing miRNA predicted targets which were negatively correlated, to a list of genes ranked according to their strength of change in expression from ICS treatment to placebo between 6 months and baseline (2). Following this analysis, the predicted targets were studied in bronchial brushings from 63 smokers with COPD and 135 control smokers without a history of using ICS or oral

corticosteroids in an independent cohort using the continuous COPD-related measurement of FEV$_1$. Genes from the independent cohort were ranked based on t-statistic values comparing patients based on their FEV1% predicted. GSEA was then utilised to investigate whether predicted miRNA gene targets of miRNAs altered both by ICS and in COPD were altered in COPD airway epithelium. A pvalue<0.05 was considered significant.

Validation in differentiated airway epithelial cells using air liquid-interface culture

Air liquid interface (ALI) culture of primary bronchial epithelial cells (PBECs) was conducted according to a previous publication (5). Briefly, PBECs obtained from suspension cultures were seeded at 75,000 in 200µl Bronchial Epithelial Cell Growth Medium (BEGM, Lonza) in the apical part of the insert and 500µl BEGM at the basolateral part. When the cell-layer was confluent (3-5 days) the cells were exposed to air at the apical side and Dulbecco's Modified Eagle Medium (DMEM) / Bronchial Epithelial Basal Medium (BEBM) (1:1) with retinoic acid (15ng/ml) added to the basolateral side (500µl). Medium was refreshed every 3 days with DMEM / BEBM (1:1) with retinoic acid (15ng/ml). Cells were quiesced on day 14 with BEBM medium for 24H and then treated with FP(10^{-8}) for 24H. Total mRNA was then collected in Tri Reagent protocol (Molecular Research Center, Inc, OH, USA) and stored at -80°C.

PCR validation

Real time PCR was conducted on total RNA obtained from ALI culture and extracted using standard Tri Reagent protocol (Molecular Research Center, Inc). Total miRNA was selectively converted using miScript II RT Kit (Qiagen), with primers for miR-320d, miR-

339-3p and miR-708 and the housekeeping RNA RNU49. RT-PCR was conducted using

Taqman primer system (Life Technologies), using an ABI7900HT PCR machine (Applied

Biosystems).

NF-κB activity assay

Human bronchial epithelial BEAS-2B cells were cultured as described previously (6). For

transfection, cells were seeded in duplicates in RPMI/5% FBS at $1x10^5$ in 24-well plates.

After 24 hours, cells were then transfected with miR-320d mimic (1nM; Qiagen, Venlo, The

Netherlands) and non-targeting control (1nM; Qiagen) using RNAimax (Invitrogen,

Groningen, The Netherlands) and NF-κB activity plasmid and a renilla luciferase protein

control, grown to confluence, serum-deprived for 24 hours and treated with IL1B for 24

hours. Total protein was then collected for the Dual-Luciferase Reporter Assay System

(Promega, Wisconsin, USA) according to manufactures' protocol. Sample NFκB activity

measurements were corrected for renilla luciferase protein in the lysate. Cigarette smoke

extract (CSE) treatment was unable to be used in the current system as it influenced

the,Renilla plasmid, which is used as an internal to correct for transfection efficiency.

Supplementary Figures:

A

Beas2b
(n=3)

Apoptotic cells
Necrotic cells
Viable cells

B

PBEC
(n=3)

Viable cells
Apoptotic cells
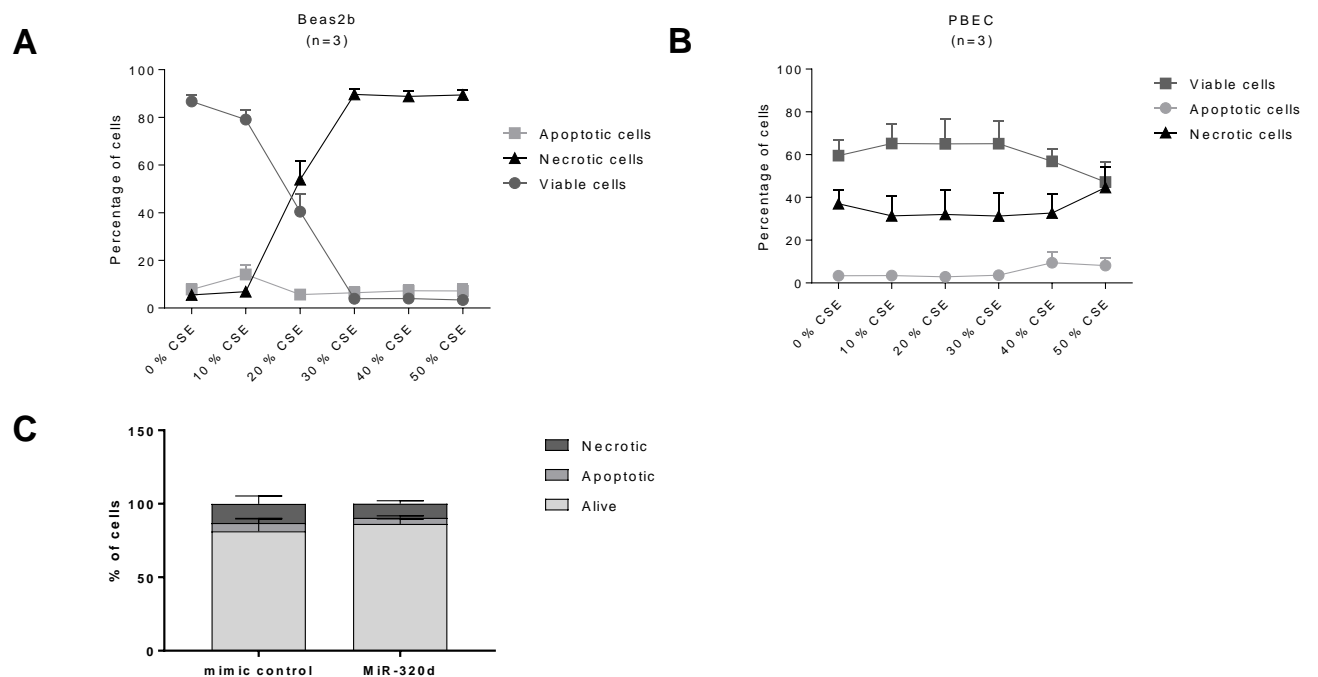Necrotic cells

C

Necrotic
Apoptotic
Alive

Fig S1. Cell viability staining. The influence of CSE exposure 0-50% of A) BEAS-2B and B) Primary Bronchial Epithelial Cells (PBEC)s and C) miR-320d overexpression on BEAS-2B. The levels of apoptotic, necrotic and viable cells were analyzed using Annexin-V/PI staining for flow cytometry.
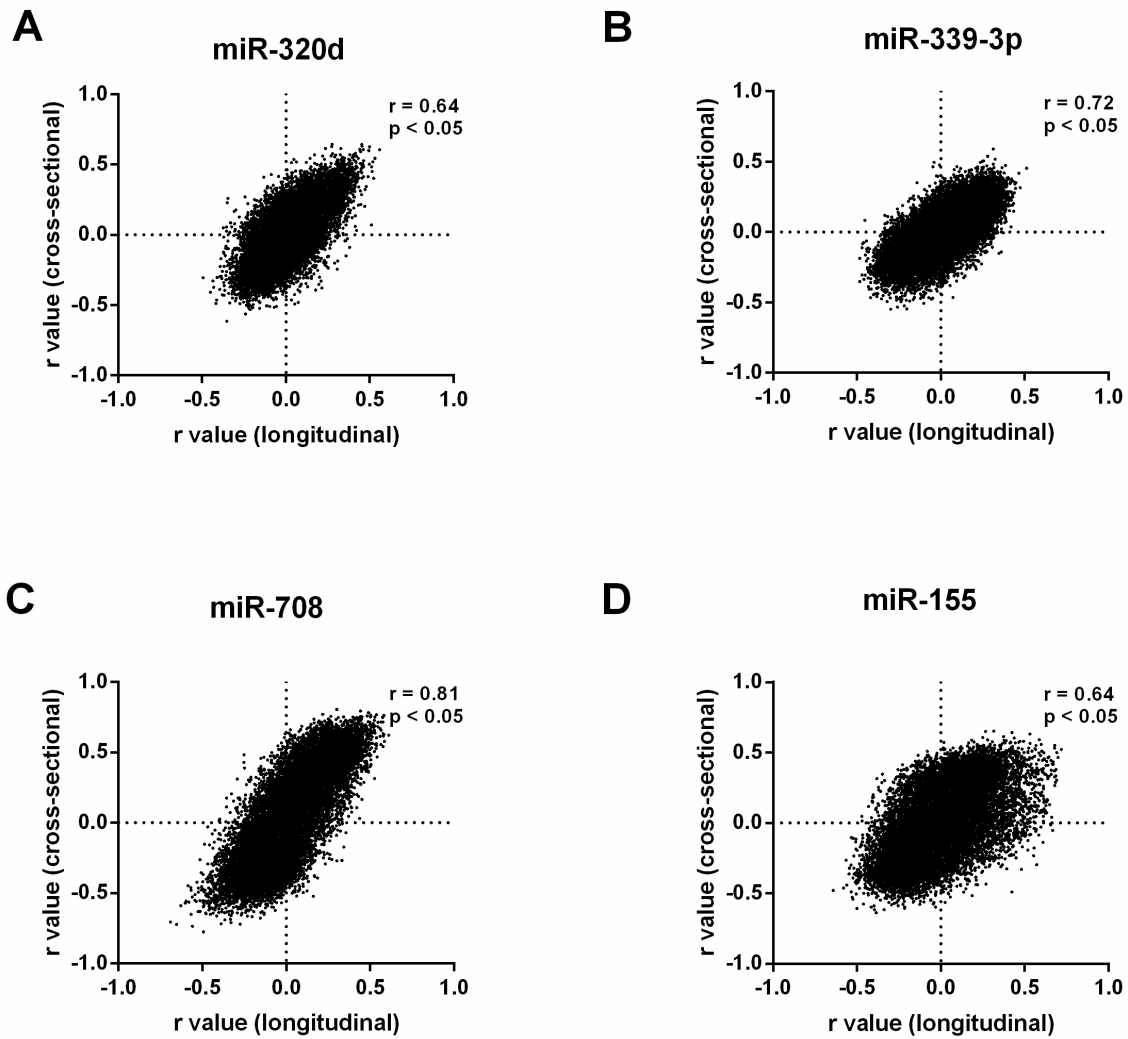
Fig. S2 Comparison between cross-sectional and longitudinal miRNA – mRNA correlation. MiRNA-mRNA Pearson correlations comparisons between cross-sectional at baseline and longitudinal analysis (6-0 months, in matched samples) for A) mir-320d, B) miR-339-3p, C) miR-708 and D) miR-155.
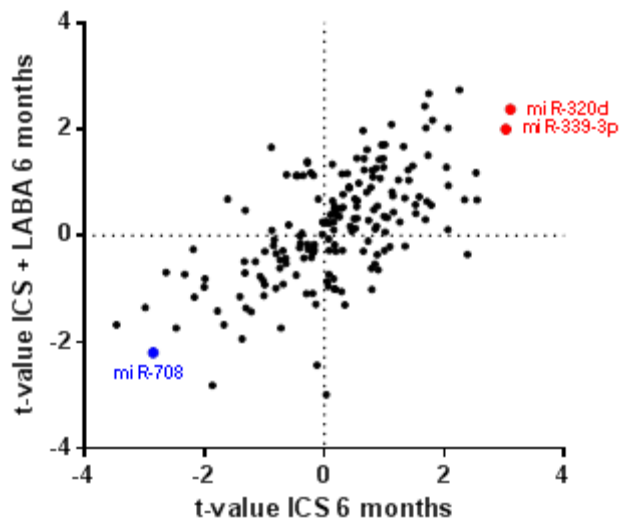
Fig. S3 Comparison of change in miRNA expression after 6 month of ICS vs placebo compared to miRNA expression after 6 month of ICS+ LABA vs placebo. Abbreviations ICS= Inhaled corticosteroids and LABA = Long-Acting Beta2-Agonists
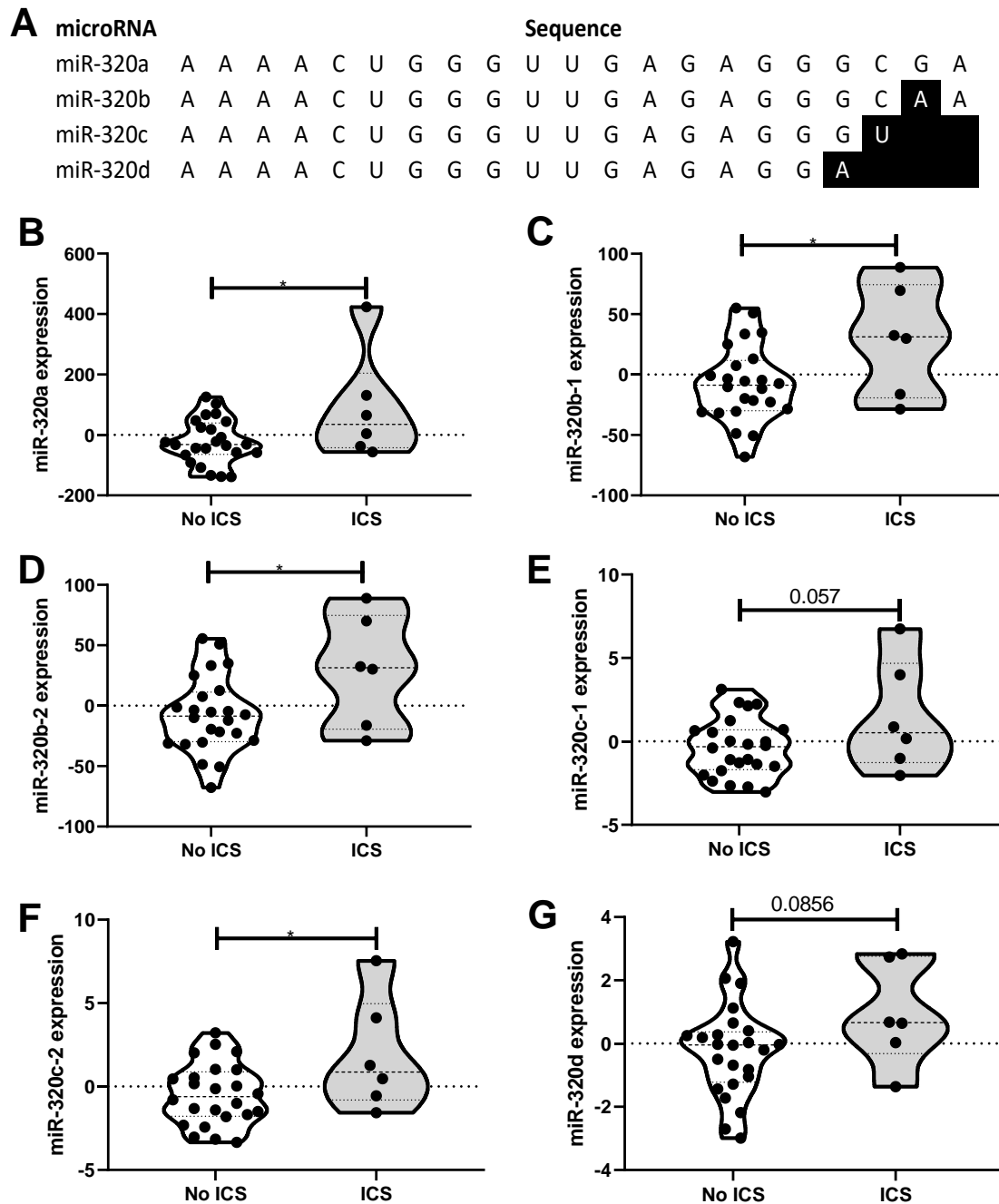
Figure S4 Replication of ICS sensitive miRNA in independent cross-sectional COPD population. A) Overlap of miR-320 family sequences MiRNA levels of bronchial brushes of COPD patients current with and without ICS treatment were measured using small RNA seq. Violin plots of B) miR-320a, C) miR-320b-1, D) miR-320b-2, E) miR-320c-1, F) miR-320c-2 and G) miR-320d. Plots show normalised gene expression counts corrected for pack years.
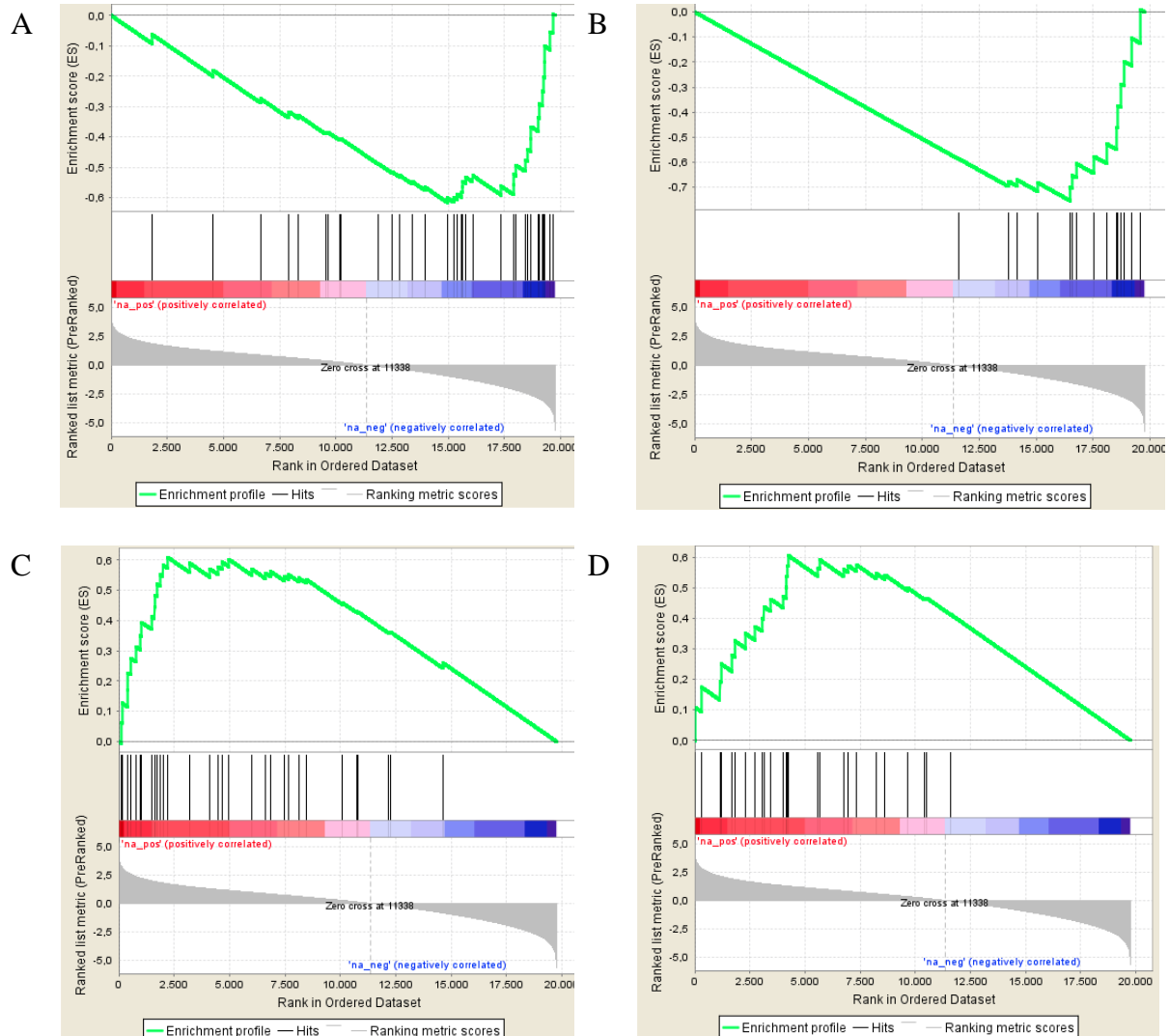
Fig S5 Gene Set Enrichment Analysis (GSEA) comparing negatively correlated miRNA predicted targets of A) miR-320d, B)miR-339-3p, C) miR-708 and D) miR-155-5p to

change in expression during 6 month ICS +/- LABA compared to placebo. The colour bar indicates the genes ranked according to their association with change in expression during 6 month ICS +/- LABA compared to placebo in bronchial biopsies (blue representing a negative association with ICS +/- LABA compared to placebo and red indicating a positive association).
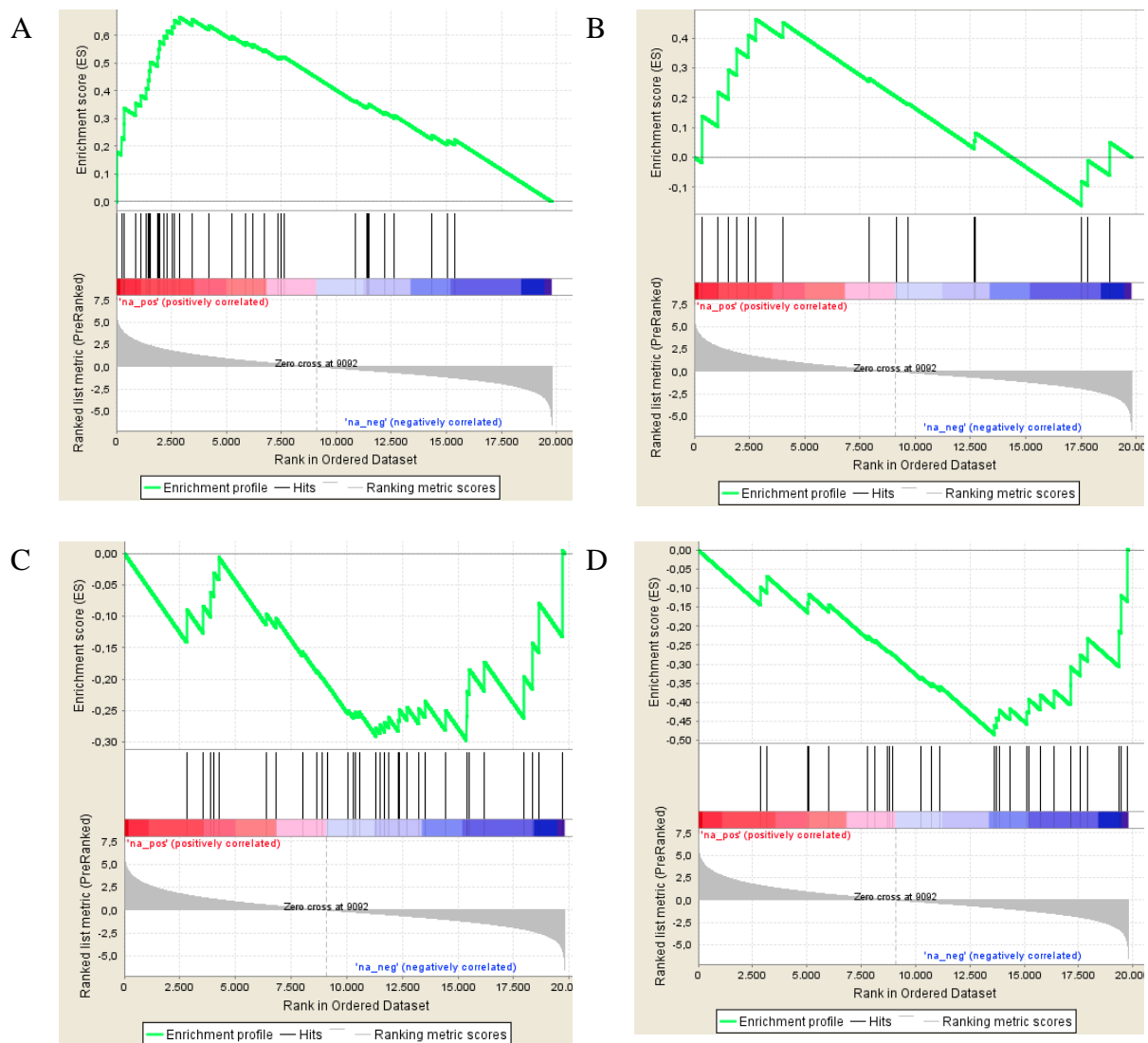
Fig S6 Gene Set Enrichment Analysis (GSEA) comparing negatively correlated miRNA predicted targets of A) miR-320d, B)miR-339-3p, C) miR-708 and D) miR-155-5p to

difference in expression between healthy and COPD bronchial brushes. The colour bar indicates the genes ranked according to their association with difference in expression between COPD and healthy bronchial brushes (blue representing a negative association between COPD and healthy bronchial brushes and red indicating a positive association).
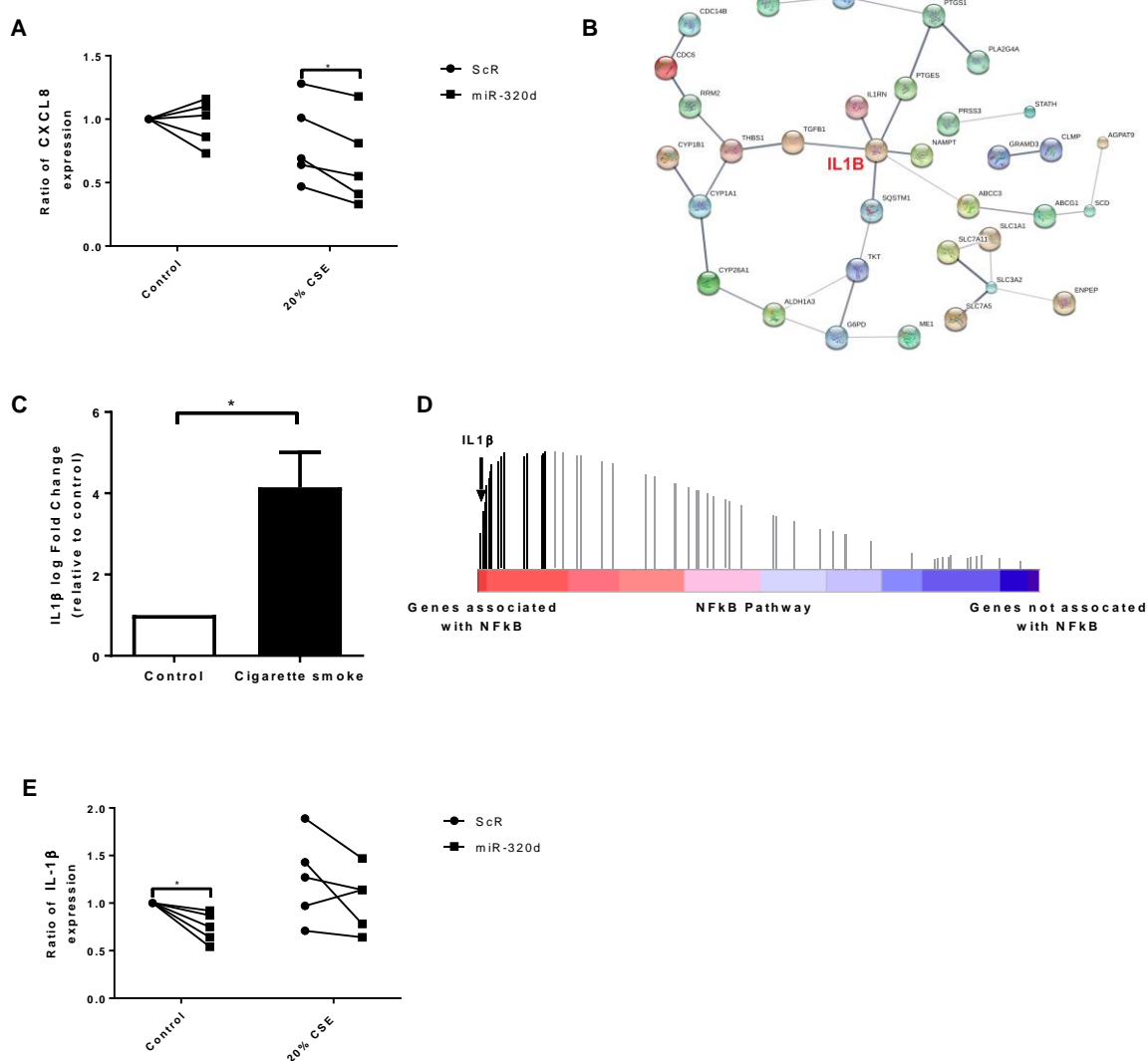

Fig. S7 Pathways altered by cigarette smoke exposure

Primary Bronchial Epithelial Cells (PBECs) were grown to confluence and hormonally-deprived overnight and transfected with non-targeting miRNA (mimic control) or miR-320d was overexpressed. A) CXCL8 mRNA expression was measured during overexpression of miR-320d mimic and scrambled control (ScR) in response to 6-hour exposure to 20 % cigarette smoke extract (CSE) (n=5). B) String network analysis of 62 genes increased (fold change> 2, FDR<0.05) in primary epithelial cells grown at ALI and treated with repeated cigarette smoke challenge (30mins exposure on four separate days), compared with no challenge. IL-1β highlighted in the red text was identified as a hub gene in this network. C) Increased expression of IL-1β in ALIs exposed to cigarette smoke. Values represent mean ± SEM. D) GSEA analysis comparing the 62 genes increased by cigarette smoke to the NF-κB pathway. This analysis found that cigarette smoke in ALI's increases the expression of genes associated with the activation of the NF-κB pathway (p<0.05).E) IL-1β mRNA expression was measured during overexpression of miR-320d mimic and scrambled control (ScR) in response to 6-hour exposure to 20 % cigarette smoke extract (CSE) (n=5). Abbreviation ALI= Air Liquid Interface, IL-1β = Interleukine-1β and GSEA= Gene Set Enrichment Analysis. All measurements were compared to A paired t-test was used to test for statistical significance. * =p<0.05

Table S2 Replication of Inhaled Corticosteroids in cross-sectional cohort of COPD patients with and without ICS treatment.

	chr	pos start	pos end	t-value	p-value
hsa-miR-320a	chr8	22102487	22102509	2.538	0.017
hsa-miR-320b-1	chr1	117214408	117214430	2.465	0.020
hsa-miR-320b-2	chr1	224444750	224444772	2.466	0.020
hsa-miR-320c-1	chr18	19263519	19263539	1.988	0.057
hsa-miR-320c-2	chr18	21901679	21901699	2.465	0.020
hsa-miR-320d	chr13	41301963	41301982	1.785	0.086

Abbreviations Chr=Chromosome, pos= position

Table S3. Top 20 Pathways associated with predicted miRNA gene targets

Pathway or process	p-value
miR-320d	
positive regulation of protein oligomerization	4 x 10-7
necrotic cell death	7 x 10-5
tumor necrosis factor-mediated signaling pathway	7 x 10-5
regulation of protein homooligomerization	10 x 10-5
regulation of protein oligomerization	10 x 10-5
cellular process involved in reproduction in multicellular organism	3 x 10-4
regulation of release of cytochrome c from mitochondria	4 x 10-4
regulation of JNK cascade	4 x 10-4
JNK cascade	4 x 10-4
release of cytochrome c from mitochondria	5 x 10-4
regulation of JUN kinase activity	5 x 10-4
positive regulation of release of cytochrome c from mitochondria	5 x 10-4
organ regeneration	9 x 10-4
positive regulation of JUN kinase activity	1 x 10-3
activation of pro-apoptotic gene products	1 x 10-3
regulation of protein serine/threonine kinase activity	2 x 10-3
regulation of stress-activated protein kinase signaling cascade	2 x 10-3
genitalia morphogenesis	2 x 10-3
chemokine production	2 x 10-3
suckling behavior	2 x 10-3
miR-339-3p	
positive regulation of transport	2 x 10-9
regulation of cellular localization	2 x 10-8
second-messenger-mediated signaling	2 x 10-8
cytosolic calcium ion transport	3 x 10-8
positive regulation of ion transport	4 x 10-8
calcium ion transport	4 x 10-8
calcium ion transport into cytosol	5 x 10-8
positive regulation of cell differentiation	6 x 10-8
regulation of secretion	6 x 10-8
elevation of cytosolic calcium ion concentration	7 x 10-8
negative regulation of transport	1 x 10-7
regulation of calcium ion transport	1 x 10-7
termination of signal transduction	1 x 10-7
regulation of homeostatic process	2 x 10-7
termination of G-protein coupled receptor signaling pathway	2 x 10-7
positive regulation of phosphorylation	2 x 10-7
negative regulation of G-protein coupled receptor protein signaling pathway	2 x 10-7
regulation of ion transport	2 x 10-7
positive regulation of protein phosphorylation	2 x 10-7
cytosolic calcium ion homeostasis	2 x 10-7

miR-708

calcium ion transport	6×10^{-29}
cellular ion homeostasis	7×10^{-29}
regulation of ion transport	1×10^{-27}
regulation of metal ion transport	5×10^{-27}
second-messenger-mediated signaling	8×10^{-27}
regulation of calcium ion transport	4×10^{-26}
regulation of phospholipase activity	4×10^{-26}
positive regulation of phospholipase C activity	2×10^{-25}
regulation of system process	5×10^{-25}
activation of phospholipase C activity	1×10^{-24}
positive regulation of lipase activity	2×10^{-24}
positive regulation of phospholipase activity	2×10^{-24}
regulation of lipase activity	3×10^{-24}
cellular metal ion homeostasis	1×10^{-23}
cellular calcium ion homeostasis	1×10^{-23}
cellular divalent inorganic cation homeostasis	2×10^{-23}
metal ion homeostasis	5×10^{-23}
divalent inorganic cation transport	1×10^{-22}
cAMP metabolic process	2×10^{-22}
blood circulation	3×10^{-22}

miR-155

viral reproduction	2×10^{-63}
nuclear transport	2×10^{-59}
nucleocytoplasmic transport	1×10^{-58}
protein targeting	8×10^{-56}
protein localization to organelle	2×10^{-54}
interspecies interaction between organisms	6×10^{-54}
positive regulation of I-kappaB kinase/NF-kappaB cascade	5×10^{-53}
regulation of I-kappaB kinase/NF-kappaB cascade	10×10^{-53}
negative regulation of cell cycle	3×10^{-51}
viral reproductive process	5×10^{-51}
I-kappaB kinase/NF-kappaB cascade	5×10^{-50}
regulation of cellular response to stress	2×10^{-49}
cell cycle arrest	1×10^{-47}
protein modification by small protein conjugation	1×10^{-45}
regulation of cell cycle arrest	1×10^{-43}
regulation of mitotic cell cycle	2×10^{-43}
regulation of cell cycle process	2×10^{-43}
RNA catabolic process	5×10^{-42}
protein modification by small protein conjugation or removal	7×10^{-42}
translation	1×10^{-41}

Table S4.   String pathway analysis

Pathway description	Observed gene count	false discovery rate
lipid metabolic process	16	0.000195
chronic inflammatory response	4	0.000614
cellular aldehyde metabolic process	5	0.000935
steroid metabolic process	8	0.000935
small molecule metabolic process	20	0.000935
arachidonic acid metabolic process	5	0.00203
response to organic cyclic compound	12	0.00257
neutral amino acid transport	4	0.00259
regulation of protein serine/threonine kinase activity	9	0.00421
terpenoid metabolic process	5	0.00431

References

1. Steiling K, van den Berge M, Hijazi K, Florido R, Campbell J, Liu G, Xiao J, Zhang X, Duclos G, Drizik E. A dynamic bronchial airway gene expression signature of chronic obstructive pulmonary disease and lung function impairment. *American journal of respiratory and critical care medicine* 2013; 187: 933-942.
2. van den Berge M, Steiling K, Timens W, Hiemstra PS, Sterk PJ, Heijink IH, Liu G, Alekseyev YO, Lenburg ME, Spira A. Airway gene expression in COPD is dynamic with inhaled corticosteroid treatment and reflects biological pathways associated with disease activity. *Thorax* 2014; 69: 14-23.
3. Grimson A, Farh KK-H, Johnston WK, Garrett-Engele P, Lim LP, Bartel DP. MicroRNA targeting specificity in mammals: determinants beyond seed pairing. *Molecular cell* 2007; 27: 91-105.
4. Fehrmann RS, Karjalainen JM, Krajewska M, Westra H-J, Maloney D, Simeonov A, Pers TH, Hirschhorn JN, Jansen RC, Schultes EA. Gene expression analysis identifies global gene dosage sensitivity in cancer. *Nature genetics* 2015.
5. Hackett T-L, de Bruin HG, Shaheen F, van den Berge M, van Oosterhout AJ, Postma DS, Heijink IH. Caveolin-1 controls airway epithelial barrier function. Implications for asthma. *American journal of respiratory cell and molecular biology* 2013; 49: 662-671.
6. Pouwels SD, Faiz A, Den Boef LE, Gras R, van den Berge M, Boezen HM, Korstanje R, Ten Hacken NH, Van Oosterhout AJ, Heijink IH. Genetic variance is associated with susceptibility for cigarette smoke-induced DAMP release in mice. *American Journal of Physiology-Lung Cellular and Molecular Physiology* 2017; 313: L559-L580.